Available online at www.sciencedirect.com
SCIENCE DIRECT
Journal of Power Sources 146 (2005) 264–269
JOURNAL OF POWER SOURCES
www.elsevier.com/locate/jpowsour

A study of novel anode material CoS_2 for lithium ion battery

J.M. Yan [a], H.Z. Huang [a], J. Zhang [a], Z.J. Liu [b], Y. Yang [a,*]

[a] State Key Laboratory for Physical Chemistry of Solid Surfaces and Department of Chemistry, Xiamen University, Xiamen 361005, PR China
[b] State Key Laboratory for Power Metallurgy Central South University, Changsha, Hunan 410083, PR China

Available online 14 June 2005

Abstract

This paper reports the study of cobalt disulfide as a promising anode material for lithium ion batteries. The crystal structure and surface morphology have been characterized by using X-ray diffraction (XRD), SEM and Brunauer–Emmett–Teller (BET) techniques. The results of XRD show that the sample is a cubic phase with a space group Pa3. The grain size of the sample was 30 μm with a special nano-structured characteristic as observed by means of SEM. Charge–discharge experiments show that the sample with 30 wt.% acetylene black at the current density of 50 mA g^{-1} has the best performance, it shows that the first discharge capacity is up to 1280 mAh g^{-1}. Ex situ XRD experiments were also carried out to determine the structural changes of delithiated/lithiated anode materials and used to analyze the reaction mechanism. Calculated Gibbs free energy change (ΔrG) and electromotive force (emf, E) values for the reaction $CoS_2 + 4Li^+ + 4e^- \rightarrow Co + 2Li_2S$ are −146 kJ mol and 1.898 V, respectively. Based on the results, a possible reaction mechanism of CoS_2 anode during intercalation of Li ions was proposed.

Keywords: Cobalt disulfide; CoS_2; Anode material; Lithium ion batteries

1. Introduction

Lithium ion batteries have rapidly been developed in the recent years because of the demand in many fields such as portable telephones, notebook computers and other communication equipments. Although it is being widely used in commercial Li ion batteries, carbonaceous materials as anode materials are insufficient to meet the needs of high energy density, high capacity and safety in future development. In a search for new anode materials to replace carbonaceous materials, there has been some interesting work have been published [1–14]. For example, nano-structured transition metal oxides [4,5] (i.e. Co_3O_4, NiO), lithium alloy [6,7] (i.e. Li–Si, Li–Sn), silicon alloy [8–10] (i.e. Mg_2Si, NiSi, $CaSi_2$), metal nitride and phosphate [11–14] (i.e. CuN_3, CoP_3) have been also studied. Brousse et al. [15] reported a new anode material SnS_2 which showed a capacity of 920 mAh g^{-1} in the first discharge process. Momma et al. [16] also studied the effect of annealing process on the performance of SnS_2. Poizot et al. [17] showed that the reaction mechanism of sulfides with Li^+ as same as that of oxides, which can be written as follows:

$$M^{n+}(X) + ne^- + nLi^+ \Leftrightarrow M^0 + nLi(X) \quad (X = S, O)$$

They have also found that $CoS_{0.89}$ material has a capacity of 2.8Li in the first cycle. However, to the best of our knowledge, there are not reports about the electrochemical study of CoS_2 in Li ion battery fields. In this work, we have studied the properties of a novel anode material CoS_2 for the first time. A high lithium storage capacity of 1280 mAh g^{-1} has been achieved for a CoS_2 electrode in the first cycle of discharge.

2. Experimental

2.1. Preparation of anode materials and structural characterization

The materials were synthesized using cobalt powder (200 mesh) deoxidized by hydrogen and sulfur powder (320 mesh)

* Corresponding author. Tel.: +86 592 2185753; fax: +86 592 2185753.
E-mail address: yyang@xmu.edu.cn (Y. Yang).

0378-7753/$ – see front matter © 2005 Elsevier B.V. All rights reserved.
doi:10.1016/j.jpowsour.2005.03.144

as raw materials, the mixture were heated in argon for 120 h in the range of 400–700 °C. The sample was characterized by powder X-ray diffraction (XRD), using a Rigaku Rotaflex D/max-C diffractometer with graphite monochromator and Cu Kα radiation operated at 40 kV and 30 mA. Data were collected in the range 10–90° using a constant scan method at 6°/min. The morphology of the samples was assessed using a scanning electron microscopy (LEO 1530 Field Emission Scanning Electron Microscope, Oxford Instrument). Brunauer–Emmett–Teller (BET) surface area measurement was also performed using a Sorptomatic 1900 system (Carlo Erber, Italy).

2.2. Electrochemical measurements

The CR2025 coin cells were fabricated to test electrochemical properties of CoS_2 powder. The working electrodes were made using different weight ratios of CoS_2 mixing different weight ratios of acetylene black, respectively. A solution containing 10 wt.% polyvinylidene fluoride (PVDF) in 1-methy l-2-pyrrolidinone (NMP) as a binder was added to the mixture to form a slurry. After ball-milling 3 h at a rotation rate of 500 rpm, the working electrodes were formed by coating the slurry onto copper foils and pressing at 20 MPa after drying 3 h in vacuum at 60 °C. The cells were assembled with the working electrode as prepared, lithium metal as counter electrode, and Celgard 2400 film as separator. The electrolyte was 1 M $LiPF_6$ in a mixture of ethylene carbonate (EC) and dimethyl carbonate (DMC) (1:1, v/v). Cell assembling was carried out in an argon-filled glove box (M Braun 100 G, Germany), where water and oxygen concentration was kept less than 1 ppm. The cells were galvanostatically charged and discharged at various current density of 50 100, 200, 400, 500 and 1000 mA g^{-1} between 0.02 and 3.0 V or at a constant current density of 50 mA g^{-1} in the voltage range of 0.02–3.0 and 3.0–1.6 V, respectively, using a home-made LAND CT2001A battery tester.

The delithiated/lithiated anode materials for ex situ XRD experiments were prepared by electrochemical delithiated/lithiated processes [18]. The coin cells were charged/discharged to different Li contents and voltage with a current of 50 mA g^{-1}. After charged and discharged, the anodes were carefully removed from the coin cells in an argon-filled glove box, and then rinsed with diethylene carbonate (DEC) to remove the residual electrolyte. The anodes were characterized by XRD after drying at room temperature in vacuum for 6 h. Data were collected in the range 30–60° using a scan method at 4°/min.

Cyclic voltammetric experiments adopted a three-electrode system and were performed using a CHI608A potenitiostat/galvanostat system (Shanghai, China). A Li foil pressed into Ni net served as the counter and reference electrodes. All of the electrolyte used in this work was 1 M $LiPF_6$ in a mixture of ethylene carbonate (EC) and dimethyl carbonate (DMC) (1:1, v/v). The scan potential ranges were chosen in the range of 0.02–3.0 and 1.6–3.0 V (versus Li/Li^+), and the potential scanning rate was 0.5 mV s^{-1}.

3. Results and discussion

In order to choose the suitable sulfide system and estimate its electrochemical properties such as charging/discharge potential plateau, we have done some thermodynamic analysis first. We calculated the standard Gibbs free energy change by simply considering a cell as conventionally described according as the mechanism proposed by Poizot et al. [17].

$$Li^0|Li^+|M_aX_b|M^0, Li_2X \quad (X = O, S)$$

The overall cell reaction is

$$M_aX_b + 2bLi^0 \rightarrow aM^0 + bLi_2X\ \Delta rG$$

Under pressure $p_0 = 0.1$ MPa and $T = 298$ K, we can calculate the Gibbs free energy change ΔrG and finally the electromotive force (emf) value E from the following formula, where F is Faraday's constant

$$\Delta rG = -nEF = -2bEF$$
$$-2yF[E^0(M_aX_b/M^0,\ Li_2X) - E^0(Li^+/Li^0)]$$
$$= \Delta rG^0 = \Delta rG$$

We calculated ΔrG and using the thermodynamic data given in the literature [19] for some compounds (Table 1). The Gibbs free energy values are negative, indicating that the reduction process is thermodynamically spontaneously feasible. Considering the calculated results, we studied some materials performances and found that CoS_2 material is one of possible anode material for Li ion batteries.

The XRD patterns of CoS_2 were shown in Fig. 1. The CoS_2 is a cubic phase with space group: Pa3 which measured

Table 1
Calculated Gibbs free energy change (ΔrG) and emf (E) values for the reaction $M_aY_b + 2bLi^0 \rightarrow bLi_2X\ \Delta rG$

Compound	ΔrG (kJ mol^{-1})	E (V)
TiO_2[a]	−233.53	0.605
MnO[a]	−199.17	1.032
FeO[a]	−317.10	1.643
NiO[a]	−346.24	1.794
CoO[a]	−347.01	1.798
Cu_2O[a]	−414.18	2.146
CuO[a]	−428.26	2.219
Fe_2O_3[b]	−941.40	1.625
Fe_3O_4[b]	−1229.40	1.592
FeS[b]	−320.53	1.661
FeS_2[b]	−674.95	1.749
NiS[b]	−341.43	1.769
NiS_2[b]	−717.23	1.858
MnS[b]	−202.50	1.049
CoS_2	−146.00	1.890
$CoS_{0.98}$	−196.65	1.727

[a] Reference [17].
[b] This work.

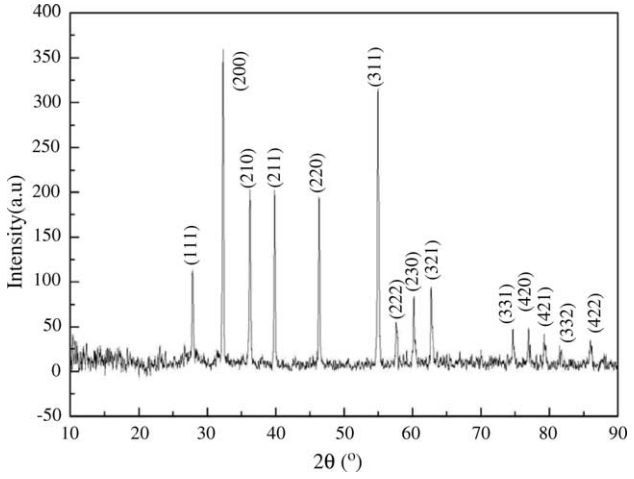

Fig. 1. The XRD patterns of CoS_2 powder.

cell parameter: $a = 5.531$Å, which is also consistent with the literature data (JCPDS card No. 41-1471).

The morphology of the CoS_2 powder was examined by using SEM. As shown in Fig. 2, the average grain size is found to be approximately 30 μm. The surface of grains has

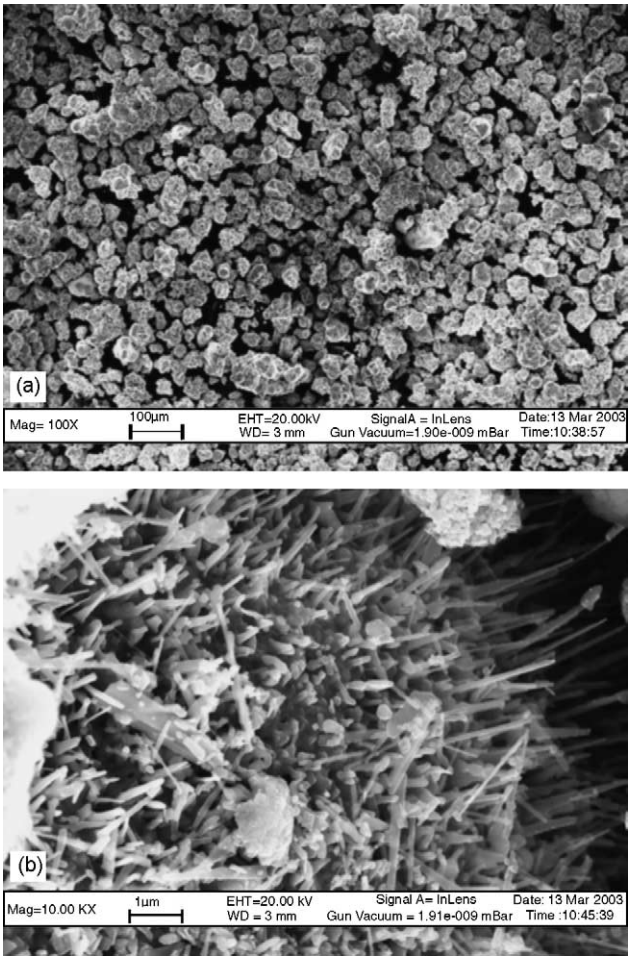

Fig. 2. SEM micrographs of CoS_2 powder.

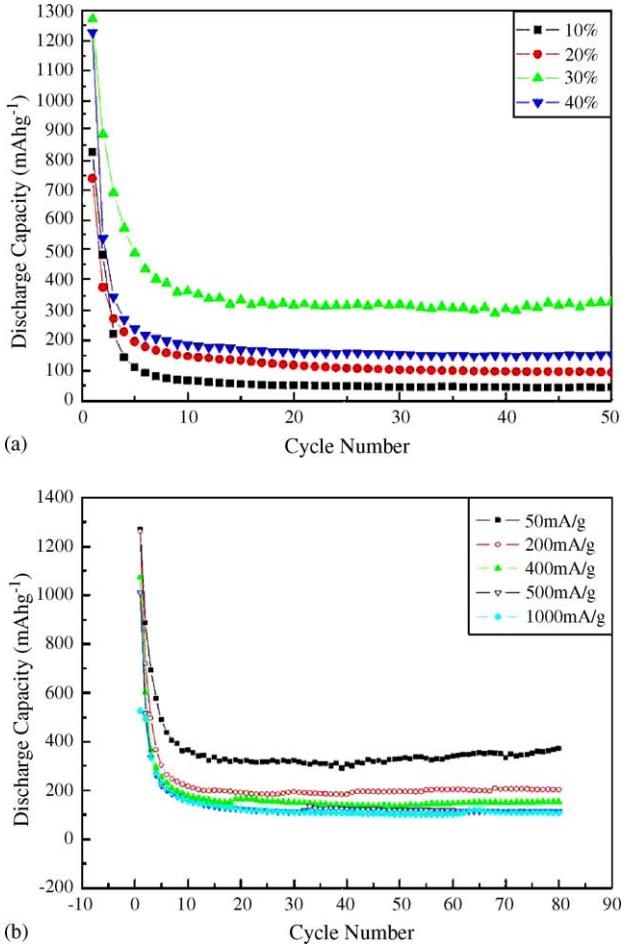

Fig. 3. The curves of discharge capacity against the cycle number of the samples: (a) with different ratios of acetylene black and (b) at various current densities.

abundant microstructure that is composed of the needle shape matter with 100 nm diameter and 2 μm length. This specific and nano-structured morphology perhaps is one of the reasons why the material facilitates to the lithiation/delithiation processes in the materials. The specific surface area was measured by BET method at 0.3 $m^2\ g^{-1}$.

It is found that the conductivity of CoS_2 material was quite low in the study of material's electrochemical performance, therefore the performance of the samples, which mixed with different contents of acetylene black were investigated. Fig. 3a shows the specific discharge capacity of the samples with different ratios of acetylene black against the cycle number in the voltage range of 0.02–3.0 V. With the ratios of acetylene black increased from 10 to 30 wt.%, the cycle performance of the materials was gradually improved, however, when the ratio of acetylene black increased to 40 wt.%, the performance of the electrode became worse. These phenomena showed that the conductance performance of CoS_2 material became better with increasing of acetylene black contents in a suitable limit, thus the electrochemical performances of the materials were also improved. When acetylene black contents were continuously increased, the

relative content of CoS_2 was decreased and the electrochemical performance of the samples were affected and deteriorated, thus the best ratio of acetylene black was 30 wt.%. With this ratio, it showed a largest discharge capacity about 1280 mAh g^{-1} when discharged to 0.02 V in the first cycle. However, the capacity decreased quickly in 10 cycles, and then kept at the level of 350 mAh g^{-1}. In addition, it was found that the first discharge capacity of the samples with other acetylene black contents was also high, but the capacity decreased to only 200 mAh g^{-1} after five cycles. With the best ratio of acetylene black, the cells were assembled and their electrochemical performances were studied at various current density. Fig. 3b shows the rate dependence of CoS_2 cycled over 0.02–3.0 V. With the current density increased, the initial discharge capacity gradually decreased and capacity fading rate was also increased. It shows that the sample with 30 wt.% different acetylene black at the current density of 50 mA g^{-1} has the best performance. In the following section, the electrochemical study of the material was based on above weight ratio and current density.

Fig. 4 shows the cyclic voltammograms for the CoS_2 electrode composed of 10 and 30 acetylene black at scan rate 0.5 mV s^{-1} in the potential range of 0.02–3 V. Three reduction peaks at 0.6, 1.2 and 1.6 V and two oxidation peaks at 2.1 and 2.5 V were observed in the first potential scanning cycle. However, the reduction peaks shifted to 1.3 and 1.8 V, the oxidation peaks shifted to 2.0 and 2.4 V in the subsequent cycles. The peak current decreased very fast as the cycle numbers increased. Thus we proposed and studied the reaction mechanism of the CoS_2 materials by an ex-situ XRD experiment. It was found that the cyclic stability of the materials have been obviously improved when scan potential range was chosen in the range of 1.6–3.0 V (shown in Fig. 4b). Only a reduction peak at about 1.7 V and two oxidation peaks at 2.0 and 2.5 V appeared in the first scan curve. In the second cycle, the reduction peak current decreased but the peak potential did not change, the oxidation peak potentials shifted to 1.9 and 2.4 V, and the current also decreased. The subsequent curves have no obvious changes. Thus, it can be seen that the cyclic stability can be greatly affected by the change of potential range. Thus, we proposed and studied the reaction mechanism of the CoS_2 materials by an ex situ XRD experiment.

Fig. 5 showed a series of the ex situ XRD patterns at different charge and discharge state. In the first discharge

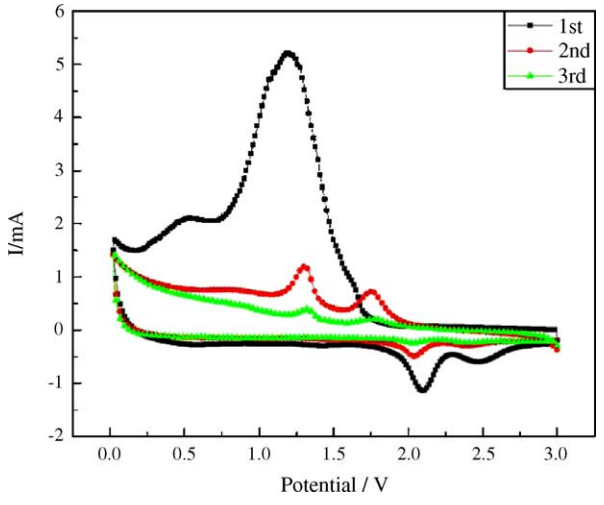

Fig. 4. Cyclic voltammograms for CoS_2 electrode composed of 10% PVDF and 30% acetylene black wi1th scan rate 0.5 mV s^{-1}. The scan potential ranges: (a) 0.02–3.0 V and (b) 1.6–3.0 V.

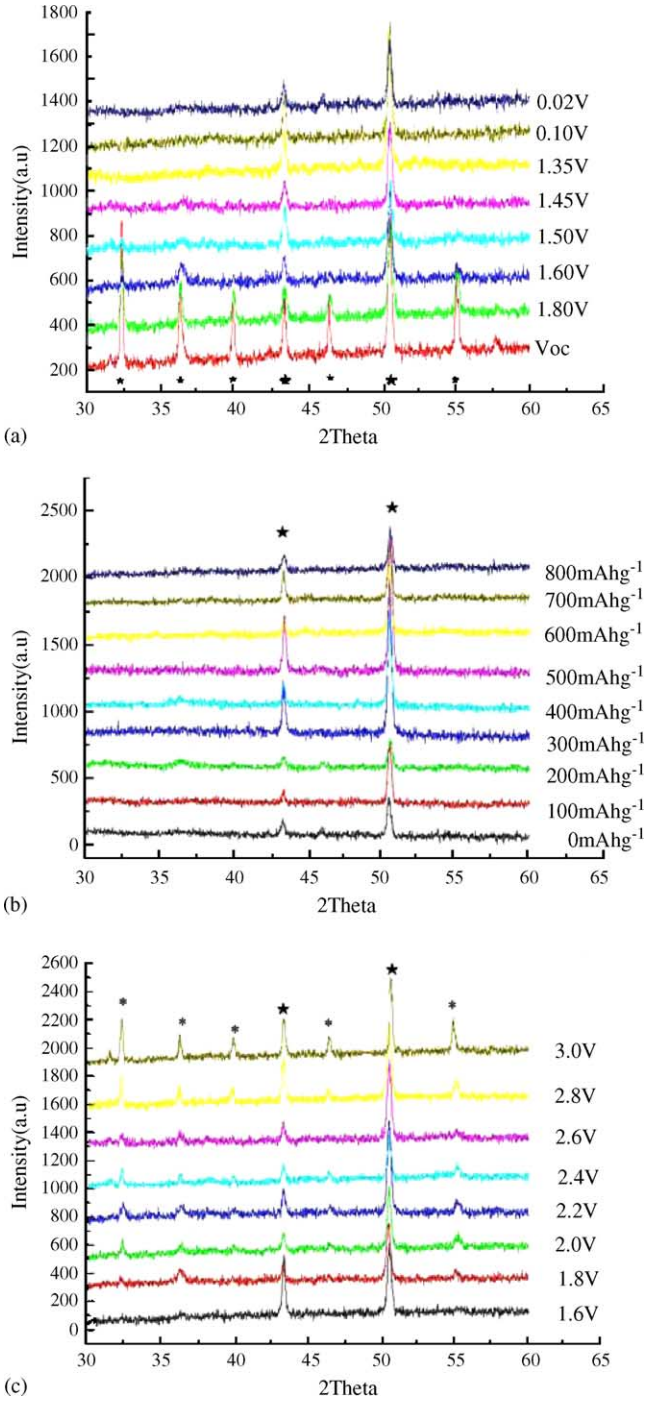

Fig. 5. The ex situ XRD figure of CoS_2 materials (★: CoS_2, ⋆: Cu substrate) (a) discharge to 0.02 V (b) charge from 0.02 V to 3.0 V (c) charge from 1.6 to 3.0 V.

Table 2
After discharged to 1.6 V, the change of cell parameters of CoS_2 material charged to different voltages

Voltage (V)	a (Å)
V_{oc}	5.532
1.8 (discharge)	5.528
1.6 (discharge)	5.527
1.8 (charge)	5.518
2.0 (charge)	5.508
2.2 (charge)	5.508
2.4 (charge)	5.518
2.6 (charge)	5.525
2.8 (charge)	5.526
3.0 (charge)	5.526

process, the main peaks of CoS_2 were still kept when the cell was discharged to 1.8 V (Fig. 5a), then the cell was discharged to 1.6 V, the main peaks of CoS_2 become weak and some peaks disappeared, it is continued to discharge to 0.02 V, no peaks except Cu substrate were observed. After discharged to 0.02 V, the cell was charged back step-by-step, as shown in Fig. 5b. During the whole charging process, the diffraction peaks of CoS_2 could not be recovered. A new cell only discharged to 1.6 V at which the diffraction peaks of CoS_2 were very weak then charged to high voltage. When charged to 1.8 V, the main peaks of CoS_2 began to appear. With the charge voltage increasing, the diffraction peaks of CoS_2 turn to be distinctive, which indicates the reproduction of cubic CoS_2 crystallites (Fig. 5c). We calculated the change of cell parameter a in the charging/discharging process, it is summarized in Table 2. The cell parameter (a) decreased during discharging process. When the cell was charged back, the values recovered while the fluctuation was small. These data suggest that the reaction the reaction in this potential region is a reversible topotactic reaction, therefore the mechanism of CoS_2 with lithium has been proposed as $xLi^+ + xe^- + CoS_2 \Leftrightarrow Li_xCoS_2$ in this voltage range. Our explanation to the above result is that the reaction is an intercalation reaction when the discharge voltage was limited at 1.6 V at that time, the frame structure of material almost was not destroyed, however, the reaction was a probable redox reaction when the discharge voltage went to lower potential (i.e. 1.6–0.02 V), then the structure of the materials was entirely destroyed at very low potential and can not be recovered. Thus, the reaction could be proposed as $CoS_2 + 4Li^+ + 4e^- \Leftrightarrow Co + 2Li_2S$. Based on the above analysis, it is expected that the charge/discharge voltage is the key factor to affect the cyclic performance, thus several cells were assembled and galvanostatically charged and discharged in the different voltage range of 3.0–1.6 and 3.0–0.02 V, respectively, in order to test their cyclic stability.

Fig. 6 illustrates charge–discharge curves of the samples in the first three cycles in different voltage range of 3.0–1.6 and 3.0–0.02 V, respectively. The first discharge curve in the voltage range 3.0–0.02 V is different from the subsequent curves (Fig. 6a) and the main difference is that it has two plateaus at 1.3 and 1.1 V, respectively, since from the second

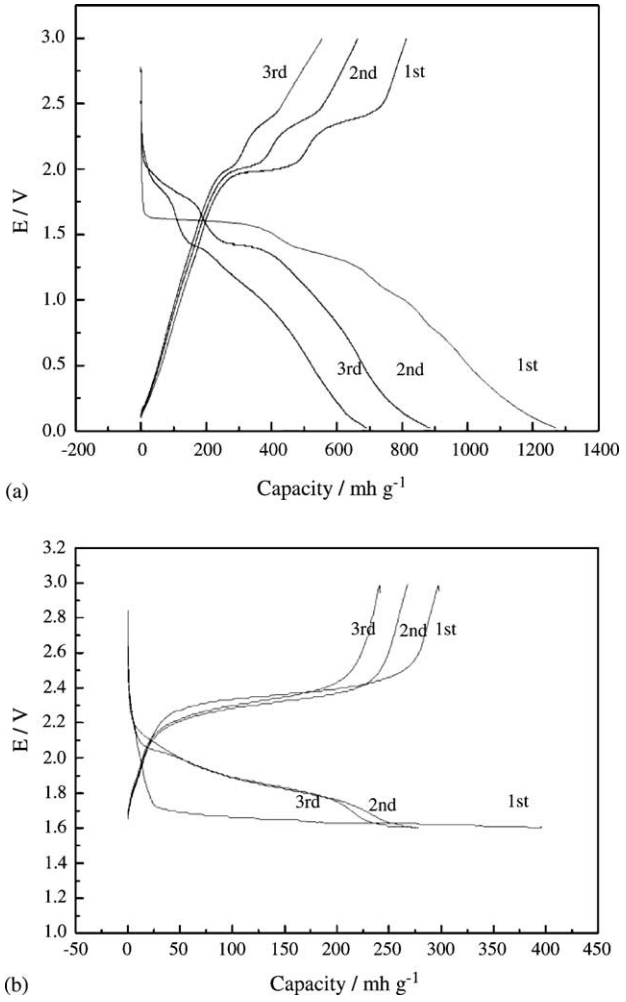

Fig. 6. Charge and discharge capacity vs. voltage curves of the electrode composed of 10% PVDF and 30% acetylene black. The charge/discharge voltage range: (a) 0.02–3 V and (b) 1.6–3.0 V.

cycle, the two plateaus shifted to 1.8 and 1.4 V, respectively. The two plateaus potentials of the charge curves were 2.0 and 2.3 V. In the voltage range 3.0–1.6 V, the first discharge curve is also different from the subsequent curves, but the capacity decay rate reduced in the following cycles. These show that the mechanisms of sample reaction are different in the different voltage ranges. Table 1 shows that the theoretical potential value is higher compared with the reduction potential of CoS_2/Li cells measured here, especially during the first discharge process. The first reduction potential of the material is about 1.6 V. Such deviation is probable due to the reaction is kinetic controlled and represents the overpotential needed to initiate and pursue the decomposition reaction.

Fig. 7 shows that the curves of the discharge capacity against the cycle number of the samples in the different voltage range 3.0–0.02 and 3.0–1.6 V. The capacity can be retained to 50.5 and 24.5% of the first discharge capacity after 20 cycles, respectively. Although the first cycle capacity of the material decreased, however, the cycling stability has been greatly improved when the voltage range changed

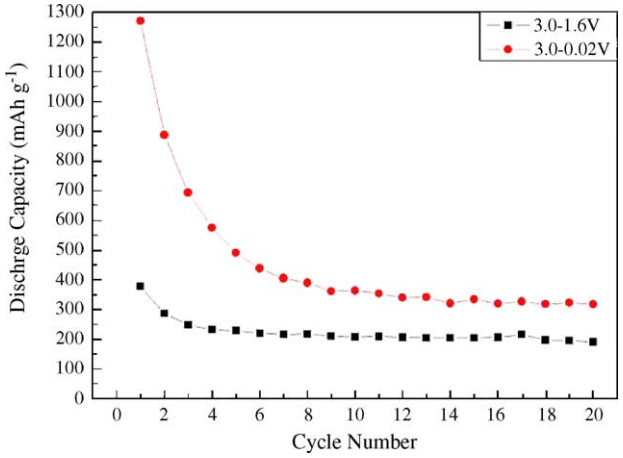

Fig. 7. The curves of discharge capacity against the cycle number of the samples in the different voltage range of 3.0–1.6 and 3.0–0.02 V.

from 3.0–0.02 to 3.0–1.6 V. This result was consistent with the above reaction mechanism analysis and also validated the mechanism proposed.

4. Conclusions

We have studied CoS_2 as a novel anode material for Li ion battery, the compound CoS_2 with cattierite structure shows larger discharge capacity than that of carbon materials in spite of the inferior capacity retention characteristics. The contents of acetylene black and the charge/discharge voltage have greatly affected to the electrochemical performance of samples. The sample with 30 wt.% acetylene black has the best performance, i.e. it showed that the first discharge capacity is about 1280 mAh g^{-1} when the cell was discharged and charged between 3.0 and 0.02 V. It is also demonstrated that the charge/discharge voltage is the key factor to affect the reaction mechanism. Based on ex situ XRD and cyclic voltammetric experimental results, it is believed that the reaction was an intercalation reaction when the discharge voltage was set at 1.6 V, the mechanism of CoS_2 with lithium has been proposed as $xLi^+ + xe^- + CoS_2 \Leftrightarrow Li_xCoS_2$. At this time, the structure of material almost was not destroyed in this reversible topotactic reaction process, however, the mechanism was redox reaction when the discharge voltage was 0.02 V, the reaction results in the collapse of the CoS_2 structure, the mechanism has been proposed as $CoS_2 + 4Li^+ + 4e^- \Leftrightarrow Co + 2Li_2S$. Calculated Gibbs free energy change (ΔrG) and emf (E) values for the reaction $CoS_2 + 4Li^+ + 4e^- \rightarrow Co + 2Li_2S$ are -146 kJ mol^{-1} and 1.898 V, respectively. In addition, due to the high discharge capacity and relatively high discharge potential plateau, the possible applications of CoS_2 as cathode materials as a potential candidate to replace FeS_2 in recently developed high energy primary Li/FeS_2 by batteries Energizer® could be expected.

Acknowledgement

This work was supported by the National Natural Science Foundation of China (Nos. 20021002, 29925310, 29833090).

References

[1] J.M. Tarascon, M. Armand, Nature 414 (2001) 359.
[2] J.L. Tirado, Mater. Sci. Eng. R 40 (2003) 103.
[3] J.O. Besenhard, M. Winter, Chemphyschemistry 3 (2002) 155.
[4] Y. Idota, T. Kubota, A. Matsufuji, Y. Maekawa, T. Miyasaka, Science 276 (1997) 1395.
[5] P. Poizot, S. Laruelle, S. Grugeon, L. Dupont, J.M. Tarascon, Nature 407 (2000) 496.
[6] L. Fang, B.V.R. Chowdari, J. Power Sources 97–98 (2001) 181.
[7] K.D. Kepler, J.T. Vaughry, M.M. Thackeray, Electrochem. Solid State Lett. 2 (1999) 307.
[8] G.X. Wang, L. Sun, D.H. Bradhurst, S. Zhang, S.X. Dou, H.K. Liu, J. Power Source 88 (2000) 278.
[9] G.A. Roberts, E.J. Cairm, H.A. Reiner, J. Power Source 110 (2002) 424.
[10] A. Netz, R.A. Huggins, W. Weppner, J. Power Source 119–121 (2003) 95.
[11] R. Niewa, F.J. Disalvo, Chem. Mater. 10 (1999) 2733.
[12] V. Pralong, D.C.S. Souza, K.T. Leung, L.F. Nazar, Electrochem. Commun. 4 (6) (2002) 516.
[13] D.C.S. Souza, V. Pralong, A.J. Jacobson, L.F. Nazar, Science 296 (2002) 2012.
[14] N. Pereira, L.C. Klein, G.G. Amatucci, J. Electrochem. Soc. 149 (2002) 262.
[15] T. Brousse, S.M. Lee, L. Pasquereau, D. Defives, D.M. Schleich, Solid State Ionics 113–115 (1998) 51.
[16] T. Momma, N. Shiraishi, A. Yoshizawa, T. Osaka, A. Gedanken, J.J. Zhu, L. Sominski, J. Power Sources 97–98 (2001) 198.
[17] P. Poizot, S. Laruelle, S. Grugeon, J.-M. Tarascon, J. Electrochem. Soc. 149 (9) (2002) 1–212.
[18] H.S. Liu, J. Li, Z.R. Zhang, Z.L. Gong, Y. Yang, Electrochim. Acta 49 (2004) 1151–1159.
[19] J.A. Dean (Ed.), Lange's Handbook of Chemistry, McGraw-Hill Book Company Press, 1975 (Section 9).